Coupling and decoupling of dual-core photonic bandgap fibers

Zhi Wang, Guiyun Kai, Yange Liu, Jianfei Liu, Chunshu Zhang, Tingting Sun, Chao Wang, Weigang Zhang, Shuzhong Yuan, and Xiaoyi Dong

Institute of Modern Optics, Nankai University, Tianjin 300071, China

Received April 28, 2005; revised manuscript received June 22, 2005; accepted June 23, 2005

Coupling characteristics of dual-core photonic bandgap fibers with triangular photonic crystal cladding are investigated by use of a vector plane-wave expansion method and a vector finite-element method. We demonstrate the eigenmodes and the coupling length for two orthogonal polarizations. A decoupling phenomenon is found at a certain wavelength in this fiber configuration. The decoupling effect is attributed to the effect of surface modes on the eigenmodes. The decoupling wavelength decreases as the ratio of core radius to cladding air-hole pitch increases from 1.05 to 1.15. © 2005 Optical Society of America

OCIS codes: 060.1810, 060.2270, 060.2280, 060.0060.

In recent years, photonic crystal fibers (PCFs) have become more attractive for their unique properties: endless single-mode guiding,[1] tailorable group-velocity dispersion,[2] and high nonlinearity.[3] According to their guided mechanisms, PCFs are generally divided into two kinds: index-guiding PCFs, which guide light by total internal reflection between a high-index core and air-hole cladding, and photonic bandgap fibers (PBGFs), which confine the light in the vicinity of the core due to the photonic bandgap (PBG) effect of photonic crystal cladding. That is, in PBGFs light can be guided in a low-index core, such as air.[4]

Owing to the remarkable flexibility in the design of PCF structure and the ease of fabricating a complex fiber structure by the stack-and-draw procedure,[5] directional couplers (DCs) based on multicore index-guiding PCFs have been widely studied in various applications, such as polarization splitters,[6–8] multiplexer–demultiplexers (MUX-DEMUXs),[9] and superbroadband DCs.[10] Recently, studies of the coupling properties of collinear air-core Bragg fibers were also presented.[11,12] However, few studies have focused on the coupling characteristics of multicore PBGFs.

Decoupling means that no power transfer occurs between adjacent waveguides. It has been proved that decoupling of parallel dielectric waveguides is possible if the index between them is an appropriate function of the transverse coordinates.[13] Recently, decoupling has been demonstrated in 2D photonic crystal slab waveguides.[14–16] However, to our knowledge, decoupling in a dual-core fiber structure has not yet been found.

In this Letter, the coupling properties of air-guided dual-core PBGFs are analyzed in detail. We demonstrate that the dispersion curves of even and odd modes propagating in dual-core PBGFs intersect and that decoupling of PBGFs takes place at the crossing point. This feature is explained by the influence of surface modes.

The designed PBGF structure is illustrated in Fig. 1. In the cross section of the PBGFs, two large air holes are introduced into the photonic crystal cladding, with a triangular lattice pattern of air holes as defect cores. The structure parameters are defined as lattice constant Λ, air-hole radius $r=0.47\Lambda$, and the radius of the two defect cores, r_c. The spacing between two cores is 3Λ. The background silica index is assumed to be 1.444, and the material dispersion of silica is neglected since the power of the guided modes in the PBGF is localized mainly in the air cores.

The guided properties of the dual-core PBGF are investigated by use of the full-vector plane-wave expansion (PWE) method and the full-vector finite-element method (FEM). We obtain the dispersion curves of the PBG edges in the perfect photonic crystal cladding by PWE. Then the effective index n_{eff} and the field distribution of the eigenmodes in the PBG are calculated by the FEM with perfectly matched layers. The geometric symmetry of PBGFs allows just one-quarter of the structure to be considered in the FEM simulation (Fig. 1).

The coupling length L_c of the dual-core PBGF is defined as

$$L_c = \pi/|\beta_e^{\,i} - \beta_o^{\,i}|, \quad i = x,y, \tag{1}$$

where $\beta_e^{\,i}$ and $\beta_o^{\,i}$ are the propagation constants of the i-polarized even and odd modes, respectively. The

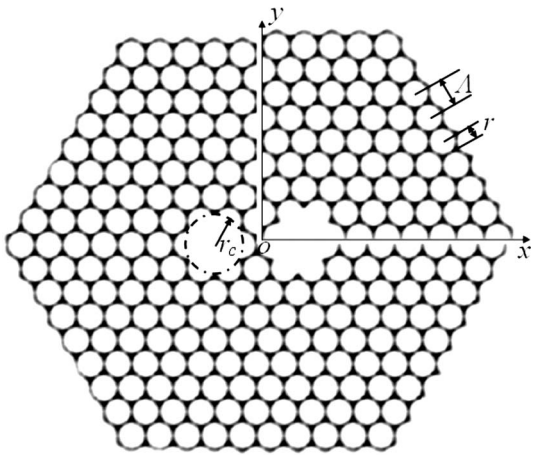

Fig. 1. Cross section of dual-core PBGF. One-quarter of the structure is considered in the FEM simulation.

0146-9592/05/192542-3/$15.00

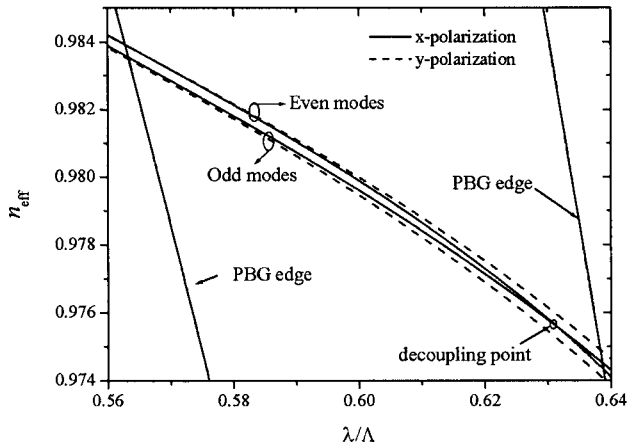

Fig. 2. Effective index of the PBG edges and the defect mode in a dual-core PBGF.

propagation constant β for the eigenmodes can be obtained from $\beta = n_{\mathrm{eff}} k$, where $k = 2\pi/\lambda$ is the vacuum wave vector and λ is the wavelength in vacuum.

Figure 2 shows the effective index n_{eff} of the guided modes and the PBG edges as a function of normalized wavelength λ/Λ with $r_c = 1.05\Lambda$. Two eigenmodes appear inside the PBG for each polarization orientation. According to the symmetry of the electrical field with respect to the y axis in Fig. 1, these modes are named even and odd modes. To ensure effective coupling operation, both the even and the odd modes should be located in the PBG region of the PBGFs where the leaky loss is low. Thus, we have acquired the following results: $0.563\Lambda \leqslant \lambda \leqslant 0.638\Lambda$ for y polarization and $0.563\Lambda \leqslant \lambda \leqslant 0.639\Lambda$ for x polarization.

Since two air cores are introduced, the counterpart modes of x and y polarization are not degenerated. In Fig. 2, for y polarization, the effective index of the even mode is higher than that of the odd mode for every wavelength, whereas for x polarization, the dispersion curves of the even and the odd modes intersect at $\lambda = 0.632\Lambda$ and the odd mode has a higher effective index than the even mode in the wavelength range over the crossing point. At the crossing point, the propagation constant of the even mode is the same as that of the odd mode and the dual-core PBGF is accordingly decoupled.

Figure 3 shows the wavelength dependence of normalized coupling length L_c/Λ for both polarization orientations. The value of L_c for y polarization gradually decreases with an increase of the wavelength, which is similar to the case of a dual-core index-guiding PCF.[9] The value of L_c for x polarization decreases slightly from $\lambda = 0.563\Lambda$ to $\lambda = 0.569\Lambda$, then increases dramatically from 869Λ at $\lambda = 0.569\Lambda$ to infinity at $\lambda = 0.632\Lambda$. The value of L_c decreases rapidly as wavelength increases in the wavelength range over the crossing point.

According to Ref. 13, decoupling occurs only when on the $x = 0$ plane

$$\int_{-\infty}^{+\infty} (E_{1y} H_{2z}^{\ *} - E_{1z} H_{2y}^{\ *}) \mathrm{d}y = 0, \qquad (2)$$

where E_{1y} and E_{1z} are y and z components of the electric field for the even mode, respectively; H_{2y} and H_{2z} are y and z components of the magnetic field for the odd mode, respectively. Equation (2) can be satisfied only when the eigenmodes are strictly vectorial modes. Due to the high refractive index difference between silica and air, the eigenmodes in PBGFs are naturally vectorial. Our numerical results show that Eq. (2) is satisfied at the decoupling point, which is in good agreement with the analytical results of Ref. 13.

The decoupling can be further explained by the effect of surface modes on the eigenmodes in the PBGF. Figure 4 shows intensity contour maps of the even and odd modes at decoupling wavelength $\lambda = 0.632\Lambda$. As shown in Fig. 4, the eigenmodes in the PBGF can be treated as combinations of Gauss-like air-core modes and surface modes[17,18] that commonly lie on the interface between the air core and the photonic crystal cladding. Because the surface modes are tightly confined to very small silica regions, the corresponding dispersion curves are steeper than the air-core modes.[19] The distribution of surface modes between two cores plays a key role in the decoupling process. For x polarization, the intensity of the surface modes in the even mode is obviously stronger than that in the odd mode, which means that the

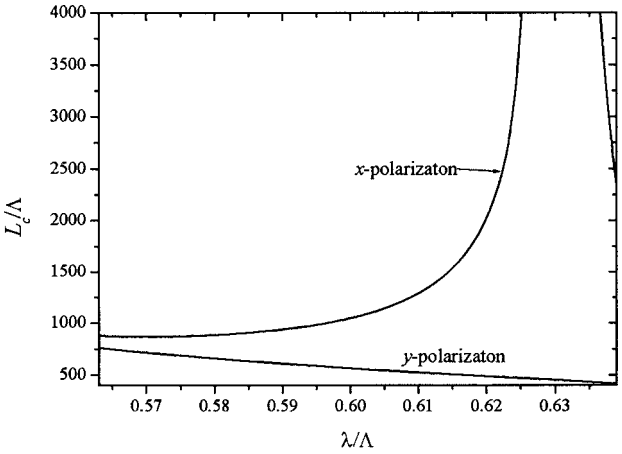

Fig. 3. Normalized coupling length of a dual-core PBGF. (The value over 4000 is not shown.)

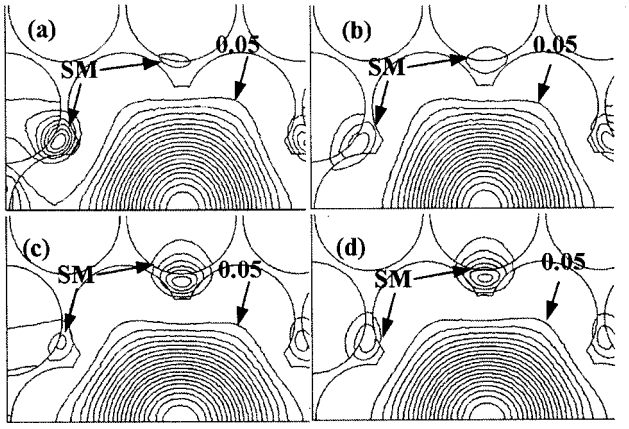

Fig. 4. Intensity contour maps of a one-quarter structure (a) even mode for x polarization, (b) odd mode for x polarization, (c) even mode for y polarization, (d) odd mode for y polarization at decoupling wavelength $\lambda = 0.632\Lambda$. The surface modes (SMs) are marked. Each contour is a 0.05 step from 0.05 to 0.95.

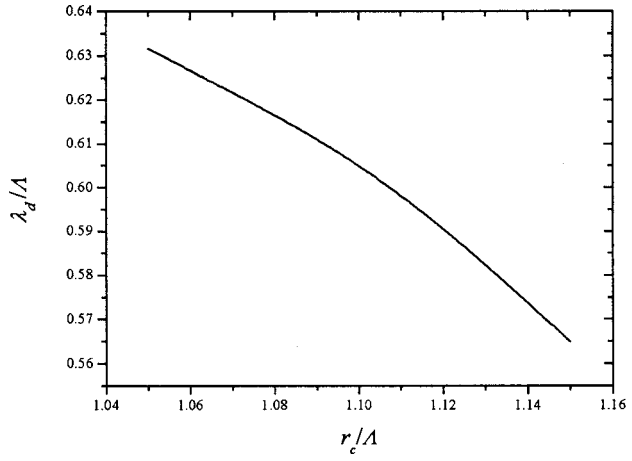

Fig. 5. Normalized decoupling wavelength λ_d/Λ as a function of normalized core radius r_c/Λ.

even mode is more strongly affected by surface modes than is the odd mode. Therefore the dispersion curve of the even mode is steeper than that of the odd mode, which induces an intersection of the dispersion curves for both modes, whereas for y polarization the intensity of the distribution of surface modes between two cores is obviously lower than that for x polarization. Therefore the surface modes in the even and odd modes do not have a significant effect on the effective index of the eigenmodes, and the decoupling does not occur at the y polarization.

Figure 5 shows the normalized decoupling wavelength λ_d/Λ as a function of normalized core radius r_c/Λ. As r_c increases from 1.05Λ to 1.15Λ, the λ_d gradually decreases. This is because the influence of the surface modes on the core-guided modes becomes stronger when r_c varies from 1.05Λ to 1.15Λ,[19,20] the dispersion curve of the even mode becomes steeper with an increase of r_c, and the crossing point of dispersion curves for even and odd modes moves toward a shorter wavelength.

In conclusion, the coupling properties of dual-core PBGF have been numerically investigated by using the PWE method and the FEM. The decoupling is found in the proposed fiber structure. In our opinion, the decoupling is because the effect of surface modes on the even mode is stronger than that on the odd mode. Around the decoupling wavelength, the coupling length for the polarization with decoupling point varies steeply and is much higher than that of the other polarization. By utilizing the above features, it is easy to design MUX–DEMUX and polarization splitter with a short fiber length. Since the power of the eigenmodes of the dual-core PBGF is distributed mainly in the air cores, this structure also has potential application in direction couplers for high-power operation.

This study was supported by the National Basic Research Program of China (973 project, grant 2003CB314906), the National 863 High Technology Project (grant 2002AA313110), and the National Science Foundation Projects (grants 60407005 and 60137010). Z. Wang's e-mail address is wangzhi@mail.nankai.edu.cn.

References

1. T. A. Birks, J. C. Knight, and P. St. J. Russell, Opt. Lett. **22**, 961 (1997).
2. J. C. Knight, J. Arriaga, T. A. Birks, A. Ortigosa-Blanch, W. J. Wadsworth, and P. St. J. Russell, IEEE Photon. Technol. Lett. **12**, 807 (2000).
3. N. G. R. Broderick, T. M. Monro, P. J. Bennett, and D. J. Richardson, Opt. Lett. **24**, 1395 (1999).
4. R. F. Cregan, B. J. Mangan, J. C. Knight, T. A. Birks, P. St. J. Russell, P. J. Roberts, and D. C. Allan, Science **285**, 1537 (1999).
5. B. J. Mangan, J. C. Knight, T. A. Birks, P. St. J. Russell, and A. H. Greenaway, Electron. Lett. **36**, 1358 (2000).
6. L. Zhang and C. X. Yang, J. Lightwave Technol. **22**, 1367 (2004).
7. L. Zhang and C. X. Yang, Opt. Express **11**, 1015 (2003).
8. K. Saitoh, Y. Sato, and M. Koshiba, Opt. Express **12**, 3940 (2004).
9. K. Saitoh, Y. Sato, and M. Koshiba, Opt. Express **11**, 3188 (2003).
10. J. Laegsgaard, O. Bang, and A. Bjarklev, Opt. Lett. **29**, 2473 (2004).
11. M. Skorobogatiy, K. Saitoh, and M. Koshiba, Opt. Lett. **29**, 2112 (2004).
12. M. Skorobogatiy, Opt. Lett. **29**, 1479 (2004).
13. G. C. Someda, Opt. Lett. **16**, 1240 (1991).
14. S. Boscolo, M. Midrio, and C. G. Someda, IEEE J. Quantum Electron. **38**, 47 (2002).
15. F. S.-S. Chien, Y.-J. Hsu, W.-F. Hsieh, and S.-C. Cheng, Opt. Express **12**, 1119 (2004).
16. Y. Tanaka, H. Nakamura, Y. Sugimoto, N. Ikeda, K. Asakawa, and K. Inoue, IEEE J. Quantum Electron. **41**, 76 (2005).
17. K. Saitoh, N. A. Mortensen, and M. Koshiba, Opt. Express **12**, 394 (2004).
18. J. A. West, C. M. Smith, N. F. Borrelli, D. C. Allan, and K. W. Koch, Opt. Express **12**, 1485 (2004).
19. H. K. Kim, J. Shin, S. H. Fan, M. J. F. Digonnet, and G. S. Kino, IEEE J. Quantum Electron. **40**, 551 (2004).
20. M. J. F. Digonnet, H. K. Kim, J. Shin, S. H. Fan, and G. S. Kino, Opt. Express **12**, 1864 (2004).